MICRO MECHANICS BASED PROGNOSIS OF PROGRESSIVE DYNAMIC DAMAGE IN ADVANCED AEROSPACE COMPOSITE STRUCTURES

Sawan Shah[1], Javid Bayandor[2], Frank Abdi[3], Ali Najafi[4]

[1]The Sir Lawrence Wackett Aerospace Centre
School of Aerospace, Mechanical and Manufacturing Engineering
Royal Melbourne Institute of Technology, Melbourne, VIC, Australia

[2]Center for Intelligent Material Systems and Structures, Virginia Tech, Blacksburg, VA, U.S.A.
E-mail: Bayandor@vt.edu

[3]Alpha STAR Corporation, Long Beach, CA, U.S.A.

[4] Center for Advanced Vehicular Systems, Department of Aerospace Engineering
Mississippi State University, Starkville, MS, U.S.A.

Keywords: *Delamination, micro-mechanics, composite structures, constitutive modelling, damage prediction*

Abstract

Analysis of advanced composites has significantly improved in recent years, leading to their successful integration into primary aerospace structures. This has been brought about by improvements in computational methodologies, primarily finite element (FE) analysis methods. However, there are particular difficulties associated with prediction of delamination using current FE approaches. The intricate architecture of fibres and matrix at the 'micro' level often cannot be captured with conventional FE techniques. Therefore, there is a growing interest in applying micro-mechanics based constitutive modelling techniques to predict damage in advanced composites. Micro/macro-mechanics approach has shown excellent accuracy and efficiency in comparison with common FE methodologies. This investigation aims to study and compare delamination prediction in a low-energy impact scenario in FE versus micro-mechanics based constitutive modelling platforms. It will be argued that through using constitutive modelling, the precision of the analysis will significantly increase without intensive calibration efforts. This form of modelling can rather easily be implemented into design and certification analyses of future advanced aerospace composite structural concepts.

1 Introduction

Advanced composite structures are finding wide-spread applications in the aerospace industry, mainly due to their high specific stiffness and strength, in addition to their improved fatigue performance, when compared to conventional aerospace-grade metallic alloys. This is further assisted by increased confidence gained through extensive developments in composite structural design, analysis and manufacture, allowing advanced composites to be used in modern commercial fleet, particularly in their primary structures [1].

Structural responses of composites to dynamic and critical loading conditions are complex. Failure in composite structures range from tensile and compressive matrix and fibre failure to delamination of the individual plies that is caused by inter and intra-laminar cracks. Composites exhibit anisotropic behaviour with generally high longitudinal and transverse strengths. However, they sustain substantial damage along the through-thickness axis due to their poor strength properties in that direction.

Accurate prediction of failure in composite structures is imperative in determining the fail-

safe flight envelops of new aircraft. Although, to this stage, a variety of failure criteria has been developed, there are still many uncertainties associated with the damage and degradation mechanisms of the composites that need to be effectively addressed. Of particular interest to aerospace manufacturers is delamination prediction, which is a common failure mode in low-to-medium energy impact events and can lead to catastrophic events in aerospace composite structures. Delamination cannot be detected visually, hence accurate prediction of its onset and specific location within laminates can prove difficult.

In low-velocity/energy impact range, delamination can occur at various locations through the thickness direction of the laminate. It is particularly common between neighbouring plies with larger different fibre orientations that translate into stiffness mismatch within the adjacent layers.

Lower impact velocities, or impacts onto relatively flexible composite laminates, result in delamination occurring predominantly near the bottom layers of the structure. This is due to higher tensile stresses induced at that location through bending. At higher velocities, the impulse during the impact occurs over a shorter time period thus resulting in the imposition of higher dynamic loading to the impact region with relatively less time for the structure to respond. Therefore, there is a greater tendency of local deformation at the impacted surface, causing the delamination to instigate immediately below the impacted surface. This is depicted in Fig.1.

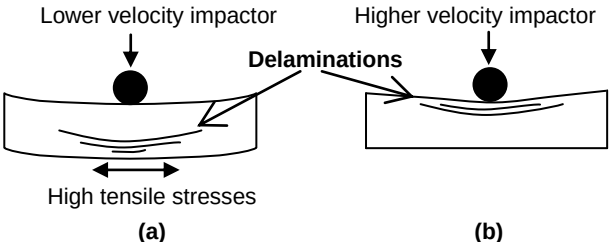

Fig.1. Delamination Caused by (a) Low and (b) Medium Energy Impacts

There are many complexities associated with physical measurement of damage in composites, including delamination initiation and growth. Computational analysis methods are being widely employed to model composite behaviour as an alternative to experimental trials.

Finite Element (FE) methods are popular in structural analyses, and have basic added features enabling them to analyse composite parts. Simple mathematical representations of various failure modes in composite structures have been developed and incorporated into commercial FE codes. However, their ability to accurately capture delamination and crack damage within composite structures is still in its infancy. This is since delamination often occurs in between constituent plies of the structure and traditionally FE codes have no or limited capability to conduct interfacial analysis.

As such, numerical capabilities continue to be developed for FE platforms and a number of more robust methodologies has been implemented into the codes to enable the delamination analysis. Within the approaches adopted, there has been an overwhelming trend to model delamination using a combination of shell and three dimensional (3D) elements. Another breakthrough has been the implementation of explicit solvers as investigated by Alfano [2], who has provided the tools with the ability to conduct non-linear analysis determining the onset of delamination. Complementing this approach, Jiang et al. [3] have proposed a method to capture damage in composite materials using interface elements.

The last decade has seen an increase in research of modelling fibre-reinforced composites with micro-mechanics based constitutive modelling approaches. These methods consider the mechanics of the material at the micro level by considering the constitutive equations of each of the constituent (fibre and matrix) phases. This differs from conventional FE methodologies that analyse the composite structures at the ply level. Unlike FE methods, the micro-mechanics based constitutive modelling approach is not mesh dependent, since it considers the stress-strain relationships at the individual constituent levels. In this methodology, the unit cell approach is adopted, whereby individual units consisting of, for example, fibre surrounded by a matrix can

be considered. In addition to FE level results that can be obtained at the ply level, the micro-mechanics modelling approach enables the unit cells to be further subdivided and analysed using constitutive equations at the micro-level, as shown in Fig.2. At this level, the micro-stress-strain relationships can be presumed sufficiently linear, hence the details of the structural responses can be established in the micro level. An automatic mesh generation feature enhances the capability of the methodology to capture progressive failure in composite structures as the failure occurs at the unit cell level. Although as discussed, the methodology is mesh independent (only a coarse mesh scheme is initially required to distribute and transfer the applied external forces down to the macro level), the automatic mesh generation feature helps effectively restrain and remove small disintegrated parts. This is executed by re-meshing the initially large elements, within which the failure has commenced, to remove the failed portions of the element. This is carried out without having to delete the element in its entirety, as premature element elimination can render the model useless.

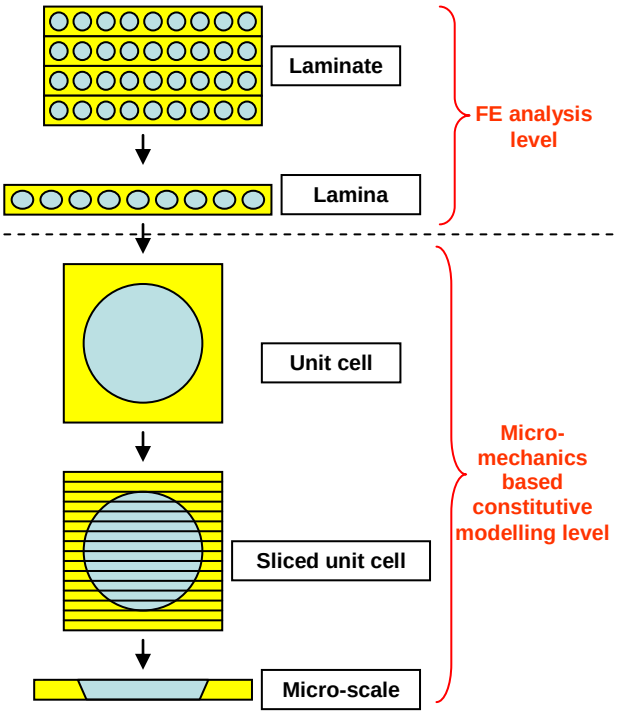

Fig.2.Enhancement of FE Analysis Results Using Micro-mechanics Based Constitutive Modelling

Using homogenisation techniques, the results from the micro scale are then used to 'build' the complete laminate up to the macro-level. Often referred to as the 'building-block' approach, this modelling strategy results in substantially quicker and more accurate solutions when compared to the conventional FE methods. More recently, high strain rate constitutive equations at the micro-mechanical level for composite materials have been defined. Xia and Xing [4] were able to identify a constitutive equation for glass-reinforced epoxy and, under strain rates of 300 s^{-1} to 2000 s^{-1}, obtained accuracies within 6% of the experimental results. Other works on the constitutive modelling approach have mostly contemplated the analysis of volumetric elements by relating them to stress-strain relationships at the micro level. Terada and Kikuchi [5] have created FE models in the micro scale by averaging the volumes from the macro level.

Micro-mechanics based constitutive modelling utilises the Material Characterisation Analysis (MCA). MCA predicts the composite lamina and laminate properties under manufacturing and environmental conditions. MCA is useful during the early phases of concept/product development. It allows evaluation of the impacts of changes in volume/void fraction involved in deciding on an appropriate fabrication approval or assessing environmental effects and degradation of material properties to environmental conditions. These conditions include the apparent moisture and thermal states of the environment in which the structure operates and manufacturing-induced characteristics such as any defects, residual strains values, etc.

MCA utilises a composite micro-mechanics scheme to compute the mechanical and physical properties of a composite with 1D, 2D or 3D fibre architecture as shown in Fig.3. An illustration of the composite modelling procedure is shown in Fig.4, where stiffness and strength as well as physical properties of each type of reinforcement, for example fillers, warps and/or through-thickness fibres, are separated into material directions based on fibre

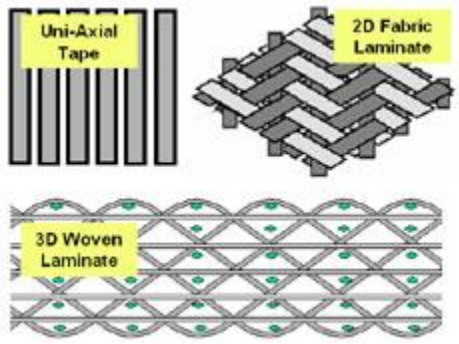

Fig.3. 1D, 2D and 3D FibreArchitecture in Composite Structures [6]

angles and contents. These are then combined with matrix properties and/or void contents to create composite unit cell properties. The modelled composite properties include stiffness, Poisson's ratios, strengths, coefficients of thermal and hygral expansion, heat conductivities and moisture diffusivities [6].

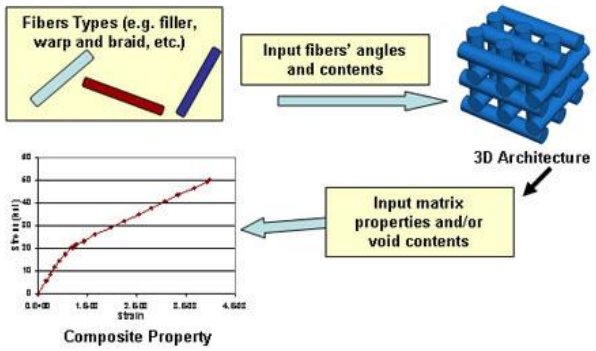

Fig.4. Micro-mechanics Modelling Procedure for Composite Structures [6]

For a structure composed of a particular material, there are fifteen variables that define the behaviour of the structure pertaining to three displacements, six strains and six stresses. In three dimensional structural models, there are a total of nine equations that can be evaluated: six kinematic equations and three equilibrium equations. Six additional equations are obtained from constitutive relations that relate the stresses to the strains. These constitutive equations vary depending on the material type from isotropic-elastic to anisotropic materials. The stress-strain relations are derived from the theory of elasticity and the basic micro-mechanics based relationships and can be used in conjunction with composite structures as summarised below [7]. Assuming the following nomenclature, and in reference to Figs 5 and 6, the geometric and mechanical relationships can be defined:

Symbols: E - Young's modulus
k - volume ratio
G - shear modulus
N_f - number of filaments per roving end
υ - Poisson's ratio
λ - weight percent
ρ - density
δ - inter-fibre, inter-ply spacing

Subscripts: m - matrix property
f - fibre property
l - ply property
v - void
1,2,3 - ply material axes

$$k_f + k_m + k_v = 1 \tag{1}$$

$$\rho_l = k_f \rho_f + k_m \rho_m \tag{2}$$

$$k_m = \frac{(1-k_v)}{1+\left(\frac{\rho_m}{\rho_f}\right)\left(\frac{1}{\lambda_m - 1}\right)} \tag{3}$$

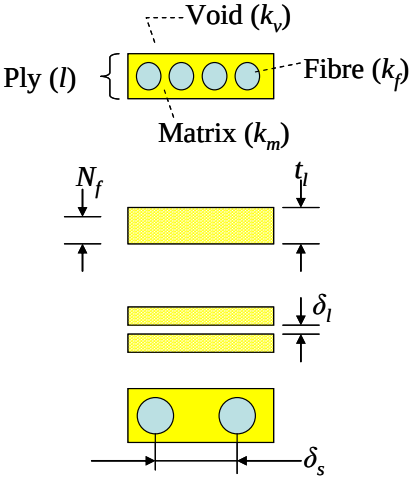

Fig.5: Geometric Relationships for Micro-mechanics of Composites

$$k_f = \frac{(1-k_v)}{1+\left(\frac{\rho_m}{\rho_f}\right)\left(\frac{1}{\lambda_f - 1}\right)} \tag{4}$$

$$\lambda_f + \lambda_m = 1 \tag{5}$$

$$t_l = \frac{1}{2}\left(N_f d_f \sqrt{\frac{\pi}{k_f}} \right) \tag{6}$$

$$\delta_l = \frac{1}{2}\left(\sqrt{\frac{\pi}{k_f}} - 2 \right) \tag{7}$$

$$\delta_s = \delta_l \tag{8}$$

For contiguous fibres:

$$k_f = \frac{\pi}{4} \approx 0.785 \tag{9}$$

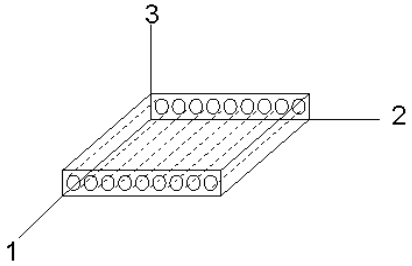

Fig.6: Ply Material Axes

$$E_{l11} = k_f E_{f11} + k_m E_m \tag{10}$$

$$E_{l22} = E_{l33} = \frac{E_m}{1 - \sqrt{k_f}\left(1 - \frac{E_m}{E_f}\right)} \tag{11}$$

$$G_{l12} = G_{l13} = \frac{G_m}{1 - \sqrt{k_f}\left(1 - \frac{G_m}{G_{f12}}\right)} \tag{12}$$

$$G_{l23} = \frac{G_m}{1 - \sqrt{k_f}\left(1 - \frac{G_m}{G_{f23}}\right)} \tag{13}$$

$$\upsilon_{l12} = \upsilon_{l13} = k_f \upsilon_{f12} + k_m \upsilon_m \tag{14}$$

$$\upsilon_{l23} = \frac{E_{l22}}{2G_{l23}} - 1 \tag{15}$$

Constitutive modelling approaches can provide up to 19 failure criteria with 8 criteria for delamination prediction, as summarised in Table 1. This accuracy of the constitutive modelling methodology in detecting and analysing failure is coupled with FE through the Progressive Failure Analyser (PFA), making the approach unique among the numerical methods [8].

To assess the strengths and weaknesses of this methodology, a low speed impact of a woven composite structure was benchmarked using a micro-mechanics based constitutive modeller. The simulation data sets were then compared with experimental results. Following this, a preliminary investigation was carried out to compare the delamination feature and results obtained from the micro-mechanics based constitutive model with the results acquired from a more common FE delamination module.

Table 1. Micro-mechanics Based Constitutive Modelling Failure Criteria for Composite Structures

Unit Cell Damage Criteria
Longitudinal tension
Longitudinal compression
Transverse tension
Transverse compression
In-plane shear (+)
In-plane shear (-)
Fibre strain limit
Modified distortion energy
Strain invariant failure theory
Normal compression
Customised criteria
Delamination Criteria
Normal tension
Transverse normal shear (+)
Transverse normal shear (-)
Longitudinal normal shear (+)
Longitudinal normal shear (-)
Relative rotation criteria
Strain Invariant Failure Theory
Discrete Cohesive Zone Model

2 Impact Problem Specifications

The low-speed impact of a 5 *in.* by 5 *in* G30-500/R6376 woven composite panel was analysed, using a micro-mechanics based constitutive modeller, and compared with experimental results. The layers were arranged in the [0/90/45/-45/90/0] lay-up with a total panel thickness of 0.084 *in.* The panel was clamped around the perimeter. A rigid spherical impactor with a diameter of 1 *in* and weight 53.75 *lbs* was used. The panel was impacted with a speed of 3.01 *ft/sec* that corresponds to

impact energy of 7.58 *ft.lbs*. The duration of the impact event was approximately 19.75 *ms*. A schematic of the impact scenario is shown in Fig.7.

Using the progressive failure dynamic analysis of the constitutive modeller, the initiation of damage at 1.6 *ms* was predicted (Fig.8). As can be observed from Fig. 9, the contact force peaked at approximately 7 *ms*, and was reduced to zero after approximately 20 *ms*. According to both the experiment and simulation, the maximum value of the contact force reached approximately 900 *lbs*. The simulated maximum deflection at the centre of the panel was 0.18 *in*, which underestimated the experimental value of 0.20 *in* by only 10 % [9].

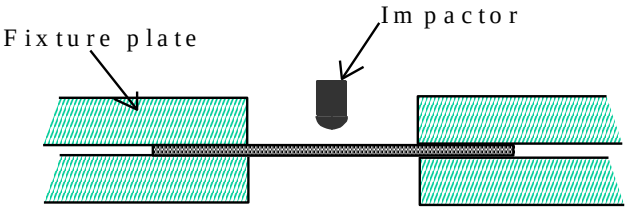

(a) Low-speed (3.01 *ft/sec*) Impact Experimental Set-up

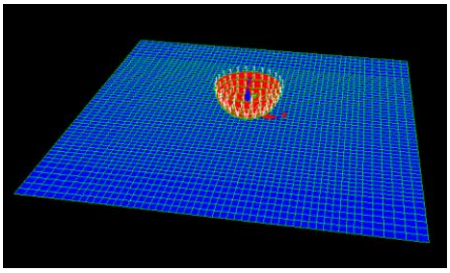

(b) Explicit FE Model

Fig.7. Impact of the Woven G30-500/R6376 Composite Panel

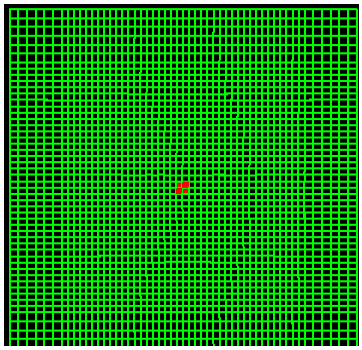

(a) Footprint Initiation Prediction at 1.6 *ms*

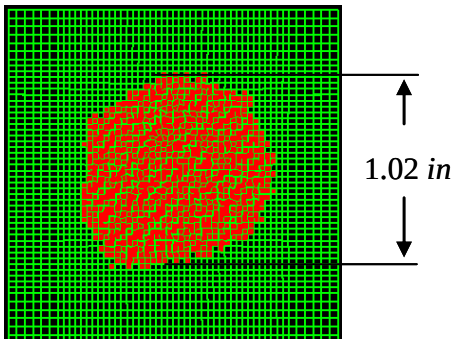

(b) Foot-print Progression Prediction at 14.1 *ms*

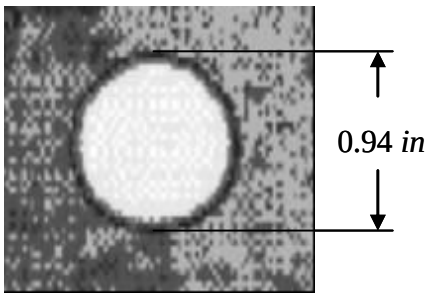

(c) Experimental Test Foot-print

Fig.8.Damage Distribution throughout the Woven Panel

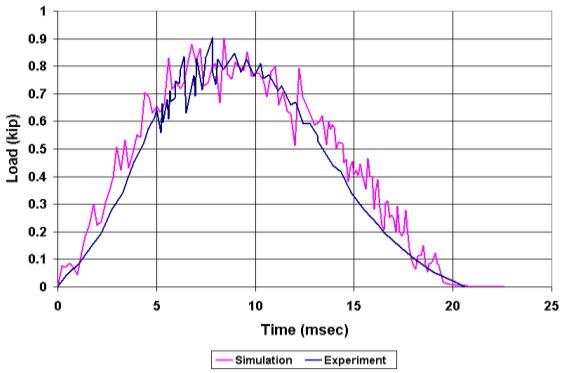

Fig.9.Comparison between Experiment and Simulation Contact Force versus Time

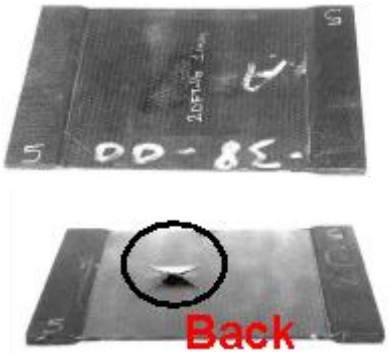

(a) Experiment: Damaged Ply (Back-face)

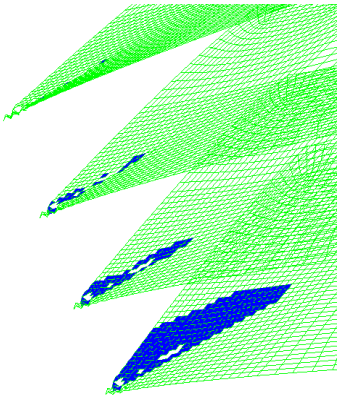

(b) Prediction of Damaged Plies

Fig.10: Comparison between Experimental and Simulated Ply Damage Using the Constitutive Modeller

As can be seen from Fig.10(b), the blue regions represent the delaminated areas between the individual plies. It was observed that the constitutive modeller gave an excellent representation of the damage experienced during the experimental test [9].

In the next step, the investigations focused on developing an FE representation to capture the delamination for a similar impact scenario in order to be compared to the constitutive modelling data. This preliminary investigation is discussed in the following section.

2.1 Composite Sandwich Impact

A foam core composite panel (11×10×0.556 *in*) was subjected to impact loads (Fig.11) from a high-speed rigid hemispherical (diameter = 1.0 *in*) piece, followed by in-plane compression until catastrophic failure of the panel [7-8]. The composite panel was made of G30-500/R3676 face-sheets of 0.056 *in* thickness with a core made of Rohacel 200W foam core, having a thickness of 0.5 *in*. Each face-sheet was made of up to four plies [0/90/-45/+45], with each ply having a thickness of 0.014 *in*. A total of 3520 shell elements was used to form the mesh for the composite panel FE model (Fig. 12) [10].

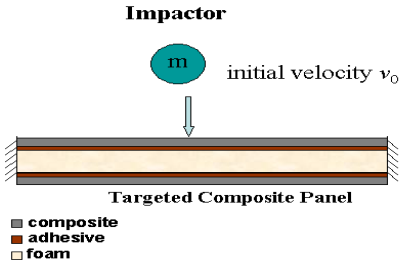

Fig.11. Schematics of the Impact on Sandwich Composite Panel

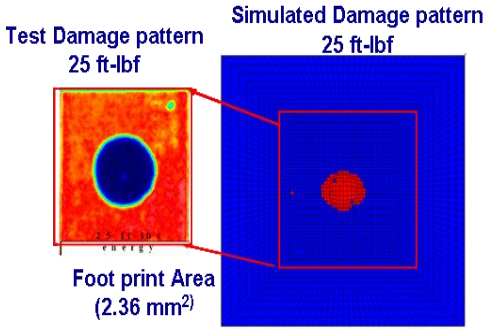

Fig. 12.Impact Foot Print Test vs. Prediction

Figure 13 shows snapshots at two intervals (2.1 and 9.6 *ms*) obtained from the FE analysis. The FE results indicate that the damage in the composite panel was initiated at 2.1 *ms* solely because of transverse out-of-plane shear stress and further accumulated because of longitudinal out-of-plane shear stress until 9.6*ms*.

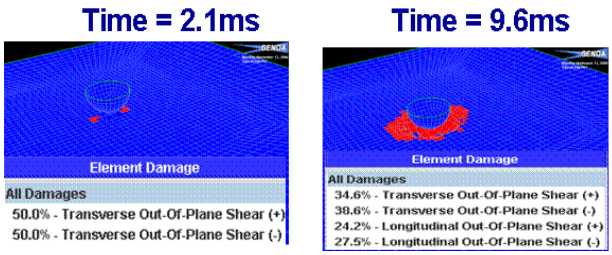

Fig. 13.Time Dependent Damage Progression and Contributing Failure Mechanisms Simulation of Impacted Composite Panel

Figure 14 shows comparison of the simulation and experimental impact energy time histories. The damage initiated at 2.1 *ms* and propagated until peak at 9.6 *ms*; thereafter, the rigid body bounced back and the contact force was reduced to zero at 20 *ms*. According to both the experiment and simulation results, the maximum value of the contact force reached was approximately 1530 *lbf*. Generally, the

predicted impact energy was consistent with that of the test.

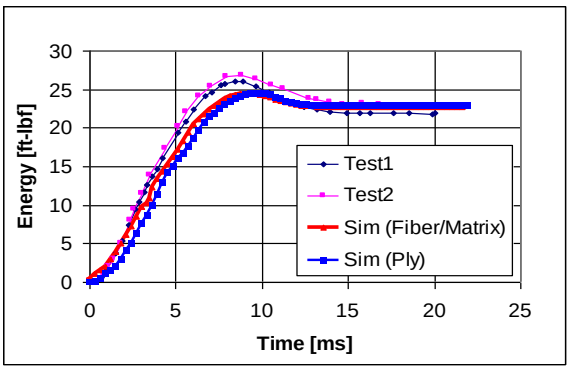

Figure 14. Impact Energy versus Time

2.2 Compression after Impact Analysis

The impacted panel was then subjected to in-plane compression using displacement control to assess the residual strength after impact. For this progressive failure static analysis, MSC Nastran was used as a stress solver. The deformed mesh, as a result of impact, along with accumulated damages and residual stresses were used as initial conditions in the compression analysis [11]. Figures 15a and 15b show the initial impacted panel and the final fractured panel subjected to compression along with the damage modes. Figure 15b indicates that the final failure of the composite panel is because of the delamination, fiber micro-buckling (crippling of bottom skins), longitudinal/transverse compression, modified distortion energy, and the previously observed out-of-plane transverse/longitudinal shear stresses. The test data indicated that the residual strength of such a panel after impact was 23.28 *kips*, with the major failure mechanism being asymmetric crippling of the bottom skin. The assessed residual strength from the progressive failure analysis was 24.68 *kips* (Fig. 15) and crippling of the bottom skin along with other failure modes. The analysis predicted residual strength of the composite panel within 6% of the test data -a reasonably well prediction for composite structures. The composite panel strength in compression was also evaluated without impact. The analysis results indicate that the overall strength was reduced by a factor of 2.25 because of the damage produced by the impact event.

3 Explicit FE Impact Model

A simplified composite panel, similar to that described earlier, was created in an FE environment. As part of the preliminary investigation, a laminate consisting of unidirectional plies was impacted at the same energy level. In this phase, due to shortcomings of the FE modelling features, unidirectional plies were used instead of woven fabric for simplification purposes. (A woven fabric model, developed separately in the micro-mechanics environment, was used to evaluate the maximum prediction accuracy possible.)

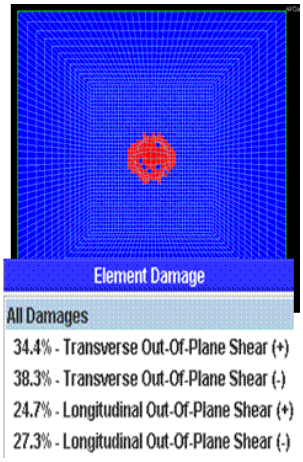

(a)

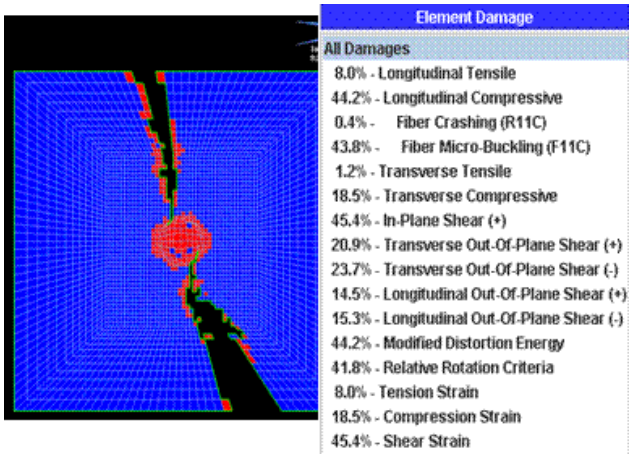

(b)

Figure 15. Damage Distribution (a) before and (b) after In-plane Compression of the Composite Panel

The unidirectional results from the constitutive modeller and FE model were compared with the aim to develop a more detailed model within the FE framework to incorporate the woven fabric composite panel representative of that described in section 2 (Fig. 16).

Type	Test	Simulation	
		Fiber/Matrix	Ply
Impact Energy (ft-lbf)	25	25	25
Impact Peak Load (lbf)	1,400	1,530	1,530
Max Deflection (in)			
CAI Residual Strength	23,280	24,136	20,707
Failure Mechanism	Asymmetric Cripplingof bottom skin	Crippling of skin (Normal Shear Failure)	Crippling of skin (Normal Shear Failure)

Figure 16. Compression after Impact (CAI) Test vs. Prediction

3.1 FE Approach

3.1.1 Model Specification

The impact scenario was simulated using explicit FE formulation using thin shell structures. The laminate edges were fully clamped. The FE model is shown in Fig. 17.

Two shells were used to model two ply 'stacks' of 0.162 *mm* thickness each, with the interface of 45/-45. For each shell element, three integration points were specified with one integration point associated with each ply. The interface between the two shells consisted of tiebreak elements that served to capture the delamination occurring between the 45° and -45° plies. This is explained in more detail in section 3.1.3.

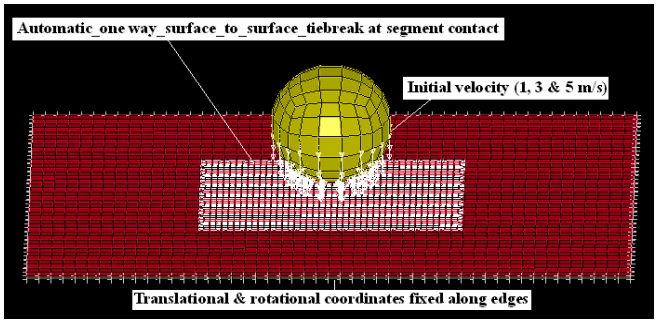

Fig. 17. Schematics of the FE Model

According to the conservation of energy, the kinetic energy of the impactor is transferred into the material upon impact in form of strain energy and damage propagation through matrix and fibre failure (heat loss during the short impact window is negligible).

The particular material model used for the composite laminates had the option of two failure criteria to capture the intra-laminar failure and damage, namely the Chang-Chang and Tsai-Wu. Of the two criteria, the Chang-Chang criterion was selected since it identifies the failure modes into fibre and matrix failure in tension and compression, whereas the Tsai-Wu criterion accounts for all the failure components into a single expression as an interactive failure criterion, thus making it difficult to identify the separate modes of failure. The associated relationships to satisfy the Chang-Chang criterion is shown below:

Tensile fibre mode:
In the tensile fibre mode, $\sigma_{11} > 0$, hence:

$$e_f^2 = \left(\frac{\sigma_{11}}{X_t}\right)^2 + \beta\left(\frac{\sigma_{12}}{S_c}\right) - 1 \begin{cases} \geq 0, \textit{failed} \\ < 0, \textit{elastic} \end{cases} \quad (16)$$

where $E_1 = E_2 = G_{12} = \upsilon_{21} = \upsilon_{12} = 0$

Compressive fibre mode:
In the compressive fibre mode, $\sigma_{11} < 0$, hence:

$$e_{cof}^2 = \left(\frac{\sigma_{11}}{X_c}\right)^2 - 1 \begin{cases} \geq 0, \textit{failed} \\ < 0, \textit{elastic} \end{cases} \quad (17)$$

where $E_1 = \upsilon_{21} = \upsilon_{12} = 0$

Tensile matrix mode:
In the tensile matrix mode, $\sigma_{22} > 0$, hence:

$$e_d^2 = \left(\frac{\sigma_{22}}{Y_t}\right)^2 + \left(\frac{\sigma_{12}}{S_c}\right) - 1 \begin{cases} \geq 0, \textit{failed} \\ < 0, \textit{elastic} \end{cases} \quad (18)$$

where $E_2 = \upsilon_{21} = 0$ and $G_{12} = 0$

Compressive matrix mode:
In the compressive matrix mode, $\sigma_{22} < 0$, hence:

$$e_d^2 = \left(\frac{\sigma_{22}}{2S_c}\right)^2 + \left[\left(\frac{Y_c}{2S_c}\right)^2 - 1\right]\frac{\sigma_{22}}{Y_c} + \left(\frac{\sigma_{12}}{S_c}\right)^2 - 1 \begin{cases} \geq 0, \textit{failed} \\ < 0, \textit{elastic} \end{cases} \quad (19)$$

where $E_1 = \upsilon_{21} = \upsilon_{12} = 0$ so that $G_{12} = 0$, and $X_c = 2Y_c$ for 50 % fibre volume.

3.1.2 Material Properties

Mechanical properties of AS4 carbon fibre/epoxy composite were used in the simulation for the laminates. This set of material data is a complete set obtained by Sandy [12] with values also available for failure strain in the trans-laminar and inter-laminar directions from an experimental test. The material properties of the rigid spherical impactor are detailed in Table 2.

Table 2. Material Properties of the Rigid Impactor

Density	7860 *kg/m*
Young's Modulus	210 *GPa*
Major Poisson's ratio	0.28
Yield strength	1.08 *GPa*

3.1.3 Delamination Criterion

Delamination is regarded as a matrix failure and two techniques were considered to capture this failure mechanism within the explicit FE environment. One methodology involved the cohesive zone modelling with interface elements that detected damage with progressive loading after reaching a specific strain energy release rate. However, limitations in computational resources resulted in the inability to accurately simulate the model using the specific cohesive elements available within the FE modeller. Therefore, the alternate approach described below was used. The analysis using the cohesive zone modelling technique was subsequently executed and is the subject of a separate document.

In the second method, delamination was captured through using surface-to-surface tiebreak contact elements. These tiebreak elements represented an adhesive link between the top and bottom shells. Within these elements, the criteria described by Eq. (20) was able to capture the delamination by scaling the normal (σ_n) and shear (σ_s) stresses in the adhesive layer of the laminate with the through-thickness failure stress (NFLS) and shear failure stresses (SFLS), respectively. A maximum allowable normal stress of $48MPa(6.96\times10^3 psi)$, allowable shear stress of $79MPa(1.15\times10^4 psi)$ and maximum normal failure strain of 0.00436 were input into the relevant data card for these contact tiebreak elements.

$$\left(\frac{|\sigma_n|}{NFLS}\right)^2+\left(\frac{|\sigma_S|}{SFLS}\right)^2\le 1 \qquad (20)$$

The above delamination criterion is illustrated in Fig. 18. At stresses above a damage scale factor of 1, the interface elements experienced plastic deformation up to a critical strain of the elements, also known as the critical crack width opening (CCRIT). Beyond this condition, the elements were no longer able to sustain strain energy, forming the region in which the in-situ of delamination was initiated.

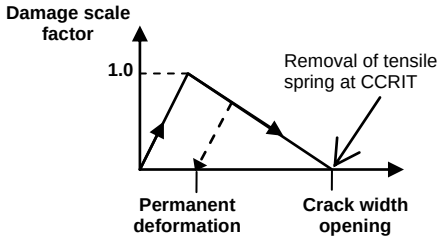

Fig. 18. Damage Profile of Contact Tiebreak Elements

Investigations indicate that delamination can occur between any of the plies. Therefore, it would have been ideal to implement the decohesion layers between all the plies in the model. Also, a single layer of shell elements representing the stack of plies would have been another preferred FE modelling option. However, the above two approaches would imply that the contact condition would have to be implemented between each of the elements as well as plies in order to capture the 3-D delamination profile, thus resulting in a computationally demanding model with an impractical solution time. For this reason, only a single contact interface with the thickness of 1 *mm* was created between the 45/-45 ply interface where maximum delamination was expected to initiate; owing to a 90° change in the fibre orientation and resulting largest stiffness mismatch between the plies. The two interfaces between the 0/90 plies were also of importance as regions of potential failure, but not included in the earlier models.

3.1.4 FE Failure Predictions

The compressive matrix failure that occurred in the impact region is depicted in Fig.19. The red regions indicate areas of the mesh where the Chang-Chang failure criterion has been met for the compressive matrix failure. Matrix failure predicted within the plies can propagate within the ply to cause inter-laminar cracking, and eventually delamination. The contour plots in Fig. 19 represent the two shells modelled displaying the results of all the integration points and hence the matrix failure for all plies. It is observed that the majority of the damage pertained to the lower plies in each shell, which reiterates the discussion in the earlier section that low-velocity impact induces high matrix stresses on the lower plies where there can be a higher probability of delamination.

There is a discontinuity of the damage distribution from the 45° to -45° plies due to the contact tiebreak elements. This highlights one of the major challenges of FE modelling and shell splitting modelling for delamination. The gap introduced between two layers of shell elements in tie contacts makes the transfer of moment loads to adjacent elements a challenging task.

Only one layer of contact tiebreak elements was used in the FE model. It is clear that if this contact layer was implemented between a different set of plies, a different damage profile would have been observed despite the fact that the total energy absorbed by the laminate would have likely remained unchanged. If there was no contact layer implemented between the shells and a single shell represented the entire laminate, there would be a more continuous damage profile between the ±45º plies, at the expense of the ability to predict delamination in that model.

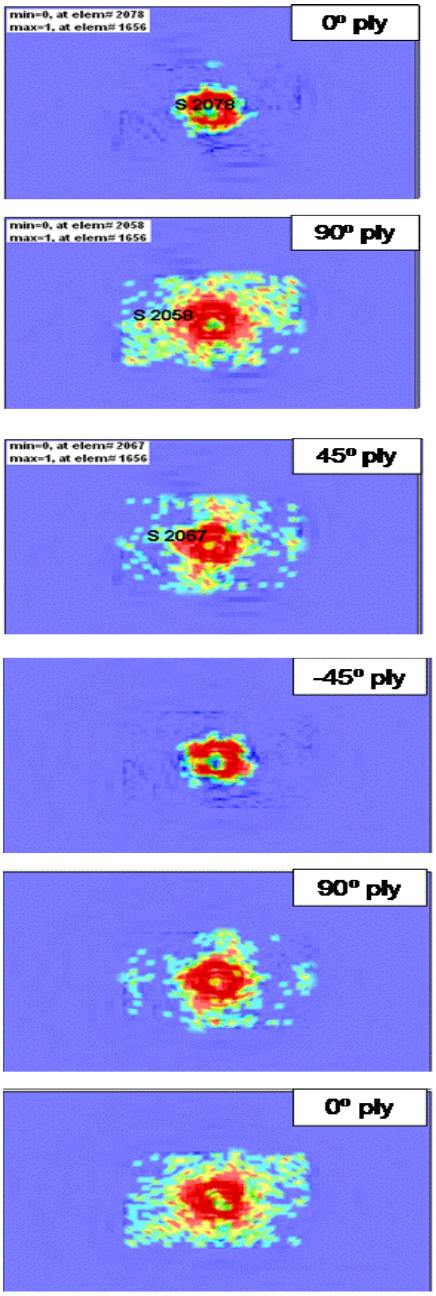

Fig. 19. Compressive Matrix Failure through all Integration Points Representing Each Ply

3.1.5 Delamination Prediction at 45°/-45° Interface

Delamination can be visually represented by analysing the variation of the contact gap between the two shells. Figure 20 shows the contact gap between the shells over the duration of the impact at three different locations. The dotted line in Fig. 20(a) approximates the delamination as captured by the tiebreak elements. Initially the gap between the adjacent shells is constant. Upon impact, there is a

variation in the contact gap and it can be seen that at points A and B, in the close vicinity of the impact region, there is a difference in the contact gap when compared to the original gap. This shows that delamination has occurred after the impact window, since the contact gap does not return to the original position over time and the laminate does not exhibit elastic behaviour. At point C, although there is a slight variation in the contact gap, the average value over the duration of the impact is approximately the same as the initial contact gap which illustrates that the delamination has not spread far away from the impact zone. A delamination profile can be obtained from this data.

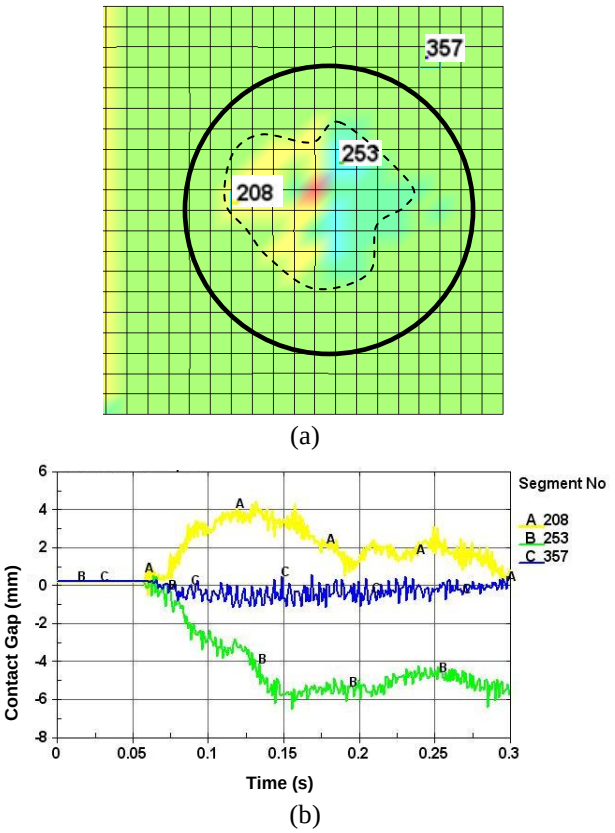

(a)

(b)

Fig. 20 (a) Contour Plot Showing Failure Region between Shells after Impact (b) Graphical Representation of Failure Region at Three Different Points on Laminate

3.2 Constitutive Modelling Approach

A similar model was simulated with a micro-mechanics based constitutive modeller. Figures 21 and 22 show a comparison between the constitutive and FE modelling results for tensile and compressive matrix failures within the ply. The red regions in the constitutive model plots are the predicted failure regions within the ply.

As can be seen in Fig. 21, the tensile failure mode is very similar in both the FE and constitutive models. The total damage profiles in the two models are also in agreement, despite the rather long horizontal region of damage initiation predicted in the FE model. This can be attributed to the absence of mesh refinement feature, an important factor that can significantly affect final simulation results. The black areas in the FE model are where elements have been eliminated. This is a limiting aspect of FE modelling and has been addressed in more detail in section 4.

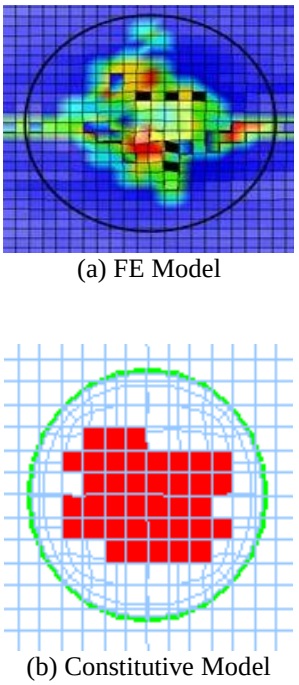

(a) FE Model

(b) Constitutive Model

Fig. 21. Tensile Matrix Failures

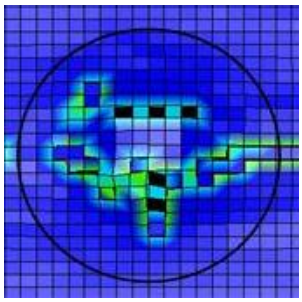

(a) FE Model

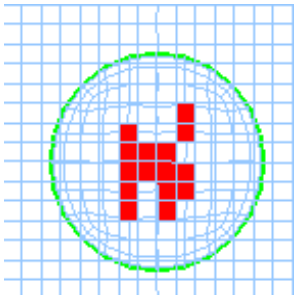

(b) Constitutive Model

Fig. 22.Compressive Matrix Failures

In comparing the tensile and compressive matrix failure results in the two modelling approaches, the FE damage appears less critical than what transpires in the constitutive model. It should be noted though that the red region in Fig. 22(b) does not necessarily indicate that the entire shaded cluster of elements has completely failed. It can also be indicative of the locations in which the damage has initiated or is progressing. Since the failure is determined based on constitutive stress-strain relationships at the micro-mechanical level, the actual failure results are independent of the mesh density. The mesh is created in the constitutive model as a means to initially absorb then distribute the external force fields, imposed on the structure, down to the macro level. Further refinement of the mesh may result in a more realistic depiction of the actual assessed damage, hence a reduced failed region. However, in micro-mechanics based constitutive modellers, the mesh refinement does not necessarily enhance the prediction accuracy achieved in the micro level.

4 Modelling Remarks

The new micro-mechanics based computational methodology for progressive failure analysis of composite structures, now imbedded in the code ASC Genoa [13], is based on the Building Block verification strategy approach that ensures an accurate simulation of the composite behavior at the micro and macro scales. This new approach was applied to the simulation of a low velocity impact onto a woven composite plate. A close agreement between the measured and simulated damage areas was achieved, including the qualitative capture of the damage state at various time intervals during the impact event.

As a preliminary investigation to evaluate the accuracy and applicability of FE analysis to predict delamination, a rather simplified version of the impacted composite plate was constructed in an explicit FE platform. The results showed part agreements with the micro-mechanics and experimental results. More accurate prediction, given the current specifications of the conventional computational facilities and FE codes, while feasible, is still optimistic.

Within the FE model, as investigated by a number of researchers [14 to 18], any change in ply orientation, hence interfacial stiffness can instigate delamination in a dynamic loading scenario. From a modelling perspective though, it is essential to simplify the model to maximise the computational efficiency. More accurate results would be achievable where additional contact layers can be incorporated within critical regions such as ply interfaces, which are likely to experience damage. This can directly affect the overall stress distribution and damage between the plies, and, perhaps offer a more realistic impression of the structural response. In this relation care must be taken since, in contrast, excessive use of contact tiebreak or decohesion elements to capture delamination can introduce susceptible regions in the laminate, where damage is bound to initiate.

A larger number of integration points could theoretically be used to better approximate the stress profile within the laminate (at the expense of computational efficiency and, sometimes, even accuracy). However, increasing the number of contact layers and shell elements as well as doubling the number of integration points within an element can render the modelling task impractical. Furthermore, the use of contact tiebreak elements and cohesive zone modelling to capture delamination can introduce discontinuity in the laminate, where damage will be bound to initiate.

To investigate the delamination occurrences at other ply interfaces within a laminate, a trial and error approach over the areas of highest stress mismatch is recommended, whereby the contact tiebreak elements are used between a different pair of adjacent elements with highest

orientation mismatch in each successive model. Although time consuming, the output from these models would give an insight into regions with highest susceptibility to delamination. Comparative plots can be obtained from the trial data to show the trends and profiles of delamination in each case.

In the FE model constructed during this study, there were often instances when certain elements were eliminated from the model as a result of the stresses within the elements exceeding the defined allowables in the material model at the individual integration points. Element elimination is particularly a problem if too many elements are removed in a narrow region. It affects the continuity of the load transfer between elements and consequently giving rise to complex shear distributions within the FE mesh. This problem is often overcome by reducing the stiffness of the element to 0, thus allowing for continuity of load transfer onto the next element; an approach adopted by constitutive modelling at the micro scale.

The effect of simplification of an FE model discounting several potentially important parameters influencing delamination, coupled with its output being highly dependent on the mesh and mesh density, largely questions the feasibility of using conventional FE techniques to predict delamination. Furthermore, FE models often require case-specific calibration, prior to which initial simulations could be up to 30 to 50% off the experimental results. In contrast, constitutive models are not overly mesh dependent (dense mesh is mostly required for high resolution visualisation purposes) and their results can be obtained through a much quicker and accurate solution, generally within 5% of the test results.

In many instances, FE modelling approach for delamination prediction in composite structures is inconclusive and has to be calibrated specifically for a particular loading condition or ply-layup. This renders it case-specific. Thus, development of more universal approaches for analysis of different scenarios, given the current computational constraints, can prove challenging.

The major benefit of micro-mechanics based constitutive methods is their capability to detect damage occurrences within multiple ply laminates. Unlike FE modelling, where integration points must be created to view the forces within a set of plies, micro-mechanics based constitutive methods allow every individual ply and their constituents to be investigated separately or together if desired.

5 Conclusion

The micro-mechanics based constitutive modelling showed excellent failure prediction when compared to an experimental test of a low-energy impact on a composite panel. To compare this method with the more conventional FE approaches, a simple FE model of a low-energy impact on a quasi-isotropic composite plate was created to predict delamination. The FE model revealed a number of analysis limitations and difficulties. Although relatively reasonable correlation was observed between the FE and the constitutive models, it appears that it is still a challenge to accurately capture delamination with an FE approach due to the numerous computational constraints that require reduced complexity of simulated composite structures. Such simplification in the FE models can in turn render the analysis of intricate structures irrelevant.

Micro-mechanics based constitutive modelling shows several promising advantages over conventional FE modelling approaches, including more accurate progressive failure analysis of composite materials. In this study, investigating failure at the micro-mechanical level quickly and more accurately led to the capture of the progressive damage within the composite, while providing a better platform to observe the nature of damage and its mechanisms. The initial investigation, using micro-mechanics based constitutive modelling approach to augment preliminary FE models, showed promising results. Future research will be directed towards a more detailed comparison of emerging FE with advanced progressive analysis features and constitutive modelling approaches.. Coupling of the two methodologies to enhance the accuracy and resolution of the results will also be carried out.

6 FutureWork

Capturing complex fibre architecture is a challenging task if carried out solely with the FE approach. Ongoing work is directed at combining the FE and constitutive modelling methods by accounting for woven fabrics and other fibre arrangements. Future work should aim to bridging the gaps in the FE analysis by augmenting it with constitutive models. This will enable the simulation processes to analyse composite laminate problems at the fibre and matrix level. By applying this approach, complex structures can be more accurately represented and determined, without any critical modelling dependencies on element sizes and mesh density. Moreover, some of the limitations of FE methodologies, highlighted in this paper, can be overcome resulting in quicker, more accurate solutions that can provide more information on the initiation and progression of inter- and intra-laminar composite damage.

7Acknowledgements

The authors would like to acknowledge the close involvement and great contribution of the researchers affiliated with this program: Messrs Damian Fratric, Jason Underwood and Do Kyun Kim.

References

[1] *High Performance Composites – Boeing sets pace for composite usage*. (Online) Available: http://www.compositeworld.com/hpc/issues/2005/86. Accessed: 5, May 2005.

[2] Alfano, G., Crisfield, M. (2001). Finite Element interface models for the delamination analysis of laminated composites. *International Journal of Numerical Methods in Engineering* 2001, 50(7): 1701-1736.

[3] Jiang W.G, Hallett S.R, and Wisnom M.R. (2004). Modelling of damage in composite materials using interface elements. *LS-Dyna User Conference.*

[4] Xia, Y. and Xing, W. (1996). *Constitutive equation for unidirectional composites under tensile impact*, Composite Science and Technology.

[5] Terada and Kikuchi (1995). Nonlinear homogenisation method for partial application. In: *Computational Methods in Micromechanics.*

[6] Alpha STAR Corporation (2007). *Composite Material Modeling with GENOA*. GENOA Bi-weekly news, Issue #8, October 4, 2007.

[7] Chamis, C. (1983). Simplified Composite Micromechanics Equations for Hygral, Thermal and Mechanical Properties. *38th Annual Conference of the Society of Plastics Industry*. Houston, Texas, February 7-11, 1983.

[8] Farahmand, B. (2000). *Fracture Mechanics of Metals, Composites, Welds, and Bolted Joints. Application of LEFM, EPFM, and FMDM Theory*, Kluwer Academic Publishers, Boston, Chap. 8.

[9] Abdi, F., Li,Q., Huang, D. and Sokolinsky, V.S. (2006). Progressive Failure Dynamic Analysis for Composite Structures. *JEC* 2006 Journal Publication

[10] Garg M. and Abumeri, G. (2007). "Assessment of Residual Strength in Impacted Composite Panels". JEC 2007 Journal Publication.

[11] Garg, M., Abdi, F., Zammit, A., Bayandor, J., Suh, Y., Song, S. (2009). "Impact Damage Resistance And Compression-After-Impact Strength Of Sandwich Composites,". *SAMPE 2009* Conference, Baltimore, MD, May 18-21.

[12] Sandy, F. (2004). *Evaluation of LS-Dyna for composite failure analysis*. RMITUniversity, Melbourne, Australia.

[13] Overview of GENOA analysis process - Alpha STAR Corporation.(OnlineWebinar), Available: www.alphastarcorp.com.

[14] Bunsell, A.R. and Renard, J. (2005). *Fundamentals of Fibre Reinforced Composite Materials*. CRC Press.

[15] Karim, M.R. (2005). *Constitutive Modelling and failure criteria of carbon-fibre reinforced polymers under high strain rates*.

[16] Bayandor, J., Abdi, F., Farahmand, B. (2008). Modelling progressive dynamic damage in advanced re-entry space transportation composite/hybrid structures. *22nd International Congress of Theoretical and Applied Mechanics.* Adelaide, South Australia, August 25-29, 2008.

[17] Garg, M., Abumeri, G.H. and Huang, D. (2008). Predicting Failure Design Envelop for Composite Material System Using Finite Element and Progressive Failure Analysis Approach. *SAMPE 2008*, Long beach, CA.

[18] Jones, R.M. (1999). *Mechanics of Composite Materials*. 2nd ed. Taylor & Francis.

Copyright Statement